Formation of Benzo[*a*]pyrene Diol Epoxide−DNA Adducts at Specific Guanines within *K-ras* and *p53* Gene Sequences: Stable Isotope-Labeling Mass Spectrometry Approach†

Natalia Tretyakova,*,‡,§ Brock Matter,‡ Roger Jones,|| and Anthony Shallop||

University of Minnesota Cancer Center, Minneapolis, Minnesota 55455, Department of Medicinal Chemistry, University of Minnesota School of Pharmacy, Minneapolis, Minnesota 55455, and Department of Chemistry, Rutgers University, Piscataway, New Jersey 08854

Received January 11, 2002; Revised Manuscript Received April 26, 2002

ABSTRACT: The mutagenicity of a prominent tobacco carcinogen, benzo[*a*]pyrene (B[*a*]P), is believed to result from chemical reactions between its diol epoxide metabolite, (+)-*anti*-7*r*,8*t*-dihydroxy-*c*9,10-epoxy-7,8,9,10-tetrahydrobenzo[*a*]pyrene (BPDE), and DNA, producing promutagenic lesions, e.g., (+)-*trans-anti*-7*R*,8*S*,9*S*-trihydroxy-10*S*-(N^2-deoxyguanosyl)-7,8,9,10-tetrahydrobenzo[*a*]pyrene (N^2-BPDE-dG). Previous studies used the DNA repair enzyme UvrABC endonuclease in combination with ligation-mediated PCR (LMPCR) to demonstrate an increased reactivity of BPDE toward guanine nucleobases within codons 157, 248, and 273 of the *p53* tumor suppressor gene (Denissenko, M. F., Pao, A., Tang, M., and Pfeifer, G. P. *Science 274*, 430−432). These sites are also "hot spots" for mutations observed in lung tumors of smokers, suggesting an involvement of B[*a*]P in the initiation of lung cancer. However, the LMPCR approach relies on the ability of the repair enzyme to excise BPDE-induced lesions, and thus the slowly repaired lesions may escape detection. Furthermore, BPDE-DNA adduct structure and stereochemistry cannot be determined. In the present work, we performed a direct quantitative analysis of N^2-BPDE-dG originating from specific guanine nucleobases within *p53*- and *K-ras*-derived DNA sequences by using a stable isotope labeling−mass spectrometry approach recently developed in our laboratory. ^{15}N-labeled dG was placed at defined positions within DNA sequences derived from the *K-ras* proto-oncogene and *p53* tumor suppressor gene, the two genes most frequently mutated in smoking-induced lung cancer. ^{15}N-labeled DNA was annealed to the complementary strands, followed by BPDE treatment and liquid chromatography−electrospray ionization tandem mass spectrometry analysis (HPLC-ESI-MS/MS) of N^2-BPDE-dG lesions. The extent of adduct formation at ^{15}N-labeled guanine was determined directly from the HPLC-ESI-MS/MS peak area ratios of ^{15}N-N^2-BPDE-dG and N^2-BPDE-dG**.** BPDE-induced guanine adducts were produced nonrandomly along *K-ras* and *p53* gene-derived DNA sequences, with over 5-fold differences in adduct formation depending on sequence context. N^2-BPDE-dG yield was enhanced by the presence of 5-Me substituent at the cytosine base-paired with the target guanine nucleobase, an endogenous DNA modification characteristic for CpG dinucleotides within the *p53* gene. In the *K-ras*-derived DNA sequence, the majority of N^2-BPDE-dG adducts originated from the first position of the codon 12 (*G*GT), consistent with the large number of G → T transversions observed at this nucleotide in smoking-induced lung cancer. On the contrary, the pattern of N^2-BPDE-dG formation within the *p53* exon 5 sequences did not correlate with the mutational spectrum in lung cancer, suggesting that factors other than N^2-BPDE-dG formation are responsible for these mutations. The stable isotope labeling HPLC-ESI-MS/MS approach described in this work is universally applicable to studies of modifications to isolated DNA by other carcinogens and alkylating drugs.

Benzo[*a*]pyrene (B[*a*]P[1]) is a prominent tobacco carcinogen likely to be involved in the initiation of lung cancer in smokers (*1*). B[*a*]P induces tumors in laboratory animals and is a suspect human carcinogen based on the similarity of B[*a*]P-DNA damage in laboratory animals and human cells (*2*). The proposed ultimate carcinogenic metabolite of B[*a*]P,

† This research was supported by research grants from the University of Minnesota Cancer Center, an American Cancer Society Institutional Grant to the University of Minnesota, the Minnesota Medical Foundation, University of Minnesota Graduate School, a developmental grant from the University of Minnesota Department of Medicinal Chemistry, and the Transdisciplinary Tobacco Use Research Center.

* To whom correspondence should be addressed.

‡ University of Minnesota Cancer Center.

§ University of Minnesota School of Pharmacy.

|| Rutgers University.

[1] Abbreviations: B[*a*]P, benzo[*a*]pyrene; BPDE, (+)-*anti*-7*r*,8*t*-dihydroxy-*c*9,10-epoxy-7,8,9,10-tetrahydrobenzo[*a*]pyrene; HPLC-ESI-MS/MS, high-performance liquid chromatography−electrospray ionization tandem mass spectrometry; LMPCR, ligation-mediated polymerase chain reaction; MALDI-TOF MS, matrix-assisted laser desorption ionization−time-of-flight detection mass spectrometry; 5-Me-C, 5-methylcytosine; N^2-BPDE-dG, (+)-*trans-anti*-7*R*,8*S*,9*S*-trihydroxy-10*S*-(N^2-deoxyguanosyl)-7,8,9,10-tetrahydrobenzo[*a*]pyrene; NNK, 4-(methylnitrosamino)-1-(3-pyridyl)-1-butanone; PAGE, polyacrylamide gel electrophoresis.

10.1021/bi025540i CCC: $22.00
Published on Web 06/27/2002

(+)-*anti*-7*r*,8*t*-dihydroxy-*c*-9,10-epoxy-7,8,9,10-tetrahydrobenzo[*a*]pyrene (BPDE), reacts with DNA to produce primarily N^2-guanine lesions, e.g., (+)-*trans*-*anti*-7*R*,8*S*,9*S*-trihydroxy-10*S*-(N^2-deoxyguanosyl)-7,8,9,10-tetrahydro benzo[*a*]pyrene (N^2-BPDE-dG) (*3*). N^2-BPDE-dG represents a strong block to DNA replication, with translesion synthesis resulting in primarily G → T transversions and a smaller percentage of G → A transition mutations (*4*−*6*).

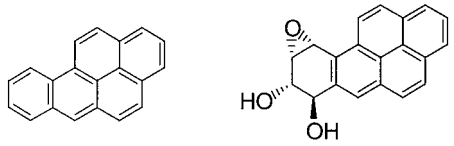

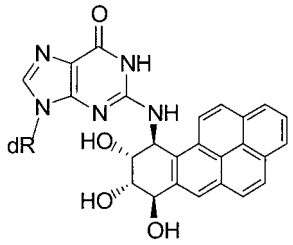

Since B[*a*]P is one of over 60 known carcinogens present in tobacco smoke, it is difficult to establish a direct relationship between tobacco B[*a*]P-induced DNA damage and mutations observed in lung cancer. Two genes most frequently mutated in smoking-induced lung tumors are the *K-ras* proto-oncogene and the *p53* tumor suppressor gene (*7*−*19*). *K-ras* is affected in 24−50% of smoking-induced lung adenocarcinoma (*7*−*12*). Sequencing analysis of *K-ras* mutants indicates that the majority of mutations are observed in codon 12, where GGT (Gly) is substituted for TGT (Cys), GTT (Val), or GAT (Asp) (*7*−*9*). These genetic changes are much more prevalent in lung cancer patients with smoking history as compared to nonsmokers (30% vs 7%), suggesting that *K-ras* codon 12 mutations result from exposure to carcinogens in tobacco smoke (*8*). The *p53* tumor suppressor gene is mutated in over 50% of nonsmall cell lung tumors (*13*−*17*, *19*−*22*). These mutations are primarily G → T transversions clustered in exons 5, 7, and 8 (*14*−*17*, *22*−*24*). Importantly, while mutations in *p53* exon 7 and 8 are shared by many tumor types, exon 5 mutations (e.g., codons 157 and 158) are characteristic for smoking induced lung cancer (*19*).

Pfeifer and co-workers have proposed that *p53* gene mutations observed in lung cancer of smokers are linked to the formation of N^2-BPDE-dG or analogous lesions with other polycyclic aromatic hydrocarbons present in tobacco smoke (*24*−*26*). These authors observed a strong correlation between the sites of increased BPDE-induced DNA damage and *p53* mutational "hot spots" (*25*). Preliminary results from the Tang group indicate a similar relationship between BPDE-dG adducts and *K-ras* mutations (*27*). Both research groups visualized the sites of BPDE-induced nucleobase lesions by analyzing DNA single-strand breaks generated by the repair enzyme, UvrABC endonuclease. The sites of modifications were mapped to specific positions in the gene by gel electrophoretic separation of LMPCR-amplified DNA fragments (*25*, *28*). While this important work suggests a direct link between PAH diol epoxide-induced DNA damage and mutations observed in lung tumors of smokers, gel electrophoresis-based methods provide only indirect information on the nature of DNA adducts. Furthermore, the quantitation of N^2-BPDE-dG by using UvrABC endonuclease-generated strand breaks may be affected by sequence-dependent repair rates of BPDE-dG lesions (*29*).

We have developed a stable isotope labeling−HPLC−electrospray ionization tandem mass spectrometry (HPLC-ESI-MS/MS) method that simultaneously provides information on the chemical identities and sequence context of carcinogen-induced nucleobase adducts. In this report, we describe the quantitative analysis of N^2-BPDE-dG adducts formed at specific guanine nucleobases within synthetic DNA oligodeoxynucleotides representing mutation-prone regions of the *K-ras* proto-oncogene and the *p53* tumor-suppressor gene. Our results indicate a nonrandom distribution of BPDE lesions in double-stranded DNA. N^2-BPDE-dG adduct formation is strongly affected by local sequence environment and is stimulated by the presence of a 5-methyl group at the cytosine nucleobase across from the target G. The pattern of N^2-BPDE-dG formation in the *K-ras* gene derived sequence containing codon 12 correlates with the frequency of G → T transversions, supporting possible involvement of this adduct or analogous lesions in the initiation of smoking-induced lung cancer. In contrast, important differences are observed between the distribution of lung cancer-associated mutations and N^2-BPDE-dG adducts within a *p53* exon 5 derived sequence.

MATERIALS AND METHODS

Caution: BPDE Is Carcinogenic and Should Be Handled with Extreme Caution. Materials. ^{15}N-dG-labeled DNA oligodeoxynucleotides representing selected regions of the *p53* tumor suppressor gene and the *K-ras* proto-oncogene (Table 1) were prepared by standard phosphoramidite chemistry using a DNA synthesizer at the University of Minnesota Microchemical Facility. ^{15}N-dG containing either three ($^{15}N_3$) or five ^{15}N atoms ($^{15}N_5$) was introduced at specified positions within oligodeoxynucleotide sequences by using ^{15}N-dG phosphoramidite prepared as described elsewhere (Shallop, A. J., Jones, R. A. Use of ^{13}C as an indirect tag in ^{15}N-labeled nucleosides. Synthesis of [8-^{13}C; 1,7-NH_2-^{15}N]-labeled adenosine, guanosine, 2′-deoxyadenosine, and 2′-deoxyguanosine. Manuscript in preparation) or purchased from Martek Biosciences (Columbia, MD). (±)-*anti*-BPDE was obtained from the NCI Chemical Carcinogen Repository (Midwest Research Institute). (±)-*anti*-D_8-BPDE was a gift from Prof. Stephen Hecht at the University of Minnesota Cancer Center.

Authentic standards of N^2-BPDE-dG and D_8-N^2-BPDE-dG were prepared by treating calf thymus DNA with (±)-*anti*-BPDE and (±)-*anti*-D_8-BPDE, respectively, as described by Barry et al. (*30*). In brief, calf thymus DNA (10 mg) was dissolved in 6 mL of 20 mM Tris-HCl buffer, pH 7, and a tetrahydrofuran solution of (±)-BPDE (1 mg in 500 μL THF) was added. Following incubation for 10 h. at 37 °C, unreacted BPDE was extracted with ethyl acetate, and the DNA was precipitated with NaCl and cold ethanol. Adducted DNA

Table 1: DNA Sequence Selected for This Study (X = ^{15}N-dG)

id	nucleotide #	sequence	calcd molecular weight	obsd molecular weight
[$^{15}N_3$]-*K-ras*-X3	211−237	GGA*X*CTGGTGGCGTAGGC	5639.7	5640.0
[$^{15}N_5$]-*K-ras*-X3	211−237	GGA*X*CTGGTGGCGTAGGC	5641.7	5642.0
[$^{15}N_3$]-*K-ras*-X4	211−237	GGAGCT*X*GTGGCGTAGGC	5639.7	5639.9
[$^{15}N_5$]-*K-ras*-X4	211−237	GGAGCT*X*GTGGCGTAGGC	5641.7	5641.4
[$^{15}N_3$]-*K-ras*-X5	211−237	GGAGCTG*X*TGGCGTAGGC	5639.7	5640.5
[$^{15}N_5$]-*K-ras*-X5	211−237	GGAGCTG*X*TGGCGTAGGC	5641.7	5641.8
[$^{15}N_3$]-*K-ras*-X6	211−237	GGAGCTGGT*X*GCGTAGGC	5639.7	5639.7
[$^{15}N_5$]-*K-ras*-X6	211−237	GGAGCTGGT*X*GCGTAGGC	5641.7	5642.0
(−)*K-ras*		GCCTACGCCACCAGCTCC	5365.5	5365.8
[$^{15}N_5$]-*p53*-exon 5-X1	1552−1570	CC*X*GCACCCGCGTCCGCG	5716.7	5716.5
[$^{15}N_3$]-*p53*-exon 5-X4	1552−1570	CCCGGCACCCGC*X*TCCGCG	5714.7	5714.6
[$^{15}N_5$]-*p53*-exon 5-X4	1552−1570	CCCGGCACCCGC*X*TCCGCG	5716.7	5716.7
[$^{15}N_3$]-*p53*-exon 5-X4, Me12	1552−1570	CCCGGCACCCG^{Me}C*X*TCCGCG	5729.7	5729.0
[$^{15}N_5$]-*p53*-exon 5-X5, Me12	1552−1570	CCCGGCACCCG^{Me}C*X*TCCGCG	5731.7	5732.8
[$^{15}N_3$]-*p53*-exon 5-X4, Me10	1552−1570	CCCGGCACCC^{Me}C*X*CGTCCGCG	5729.7	5729.0
[$^{15}N_3$]-*p53*-exon 5-X5, Me16	1552−1570	CCCGGCACCCGCGTC^{Me}C*X*CCG	5729.7	5827.7
[$^{15}N_3$]-*p53*-exon 5-X1, Me3	1552−1570	CC^{Me}C*X*GCACCCGCTCCGCG	5729.7	5729.2
(−) *p53*-exon 5		CGCGGACGCGGGTGCCGGG	5911.9	5912.0
(−) *p53*-exon 5-Me3		CG^{Me}CGGACGCGGGTGCCGGG	5926.9	5926.0
(−) *p53*-exon 5-Me7		CGCGGA^{Me}CGCGGGTGCCGGG	5926.9	5925.9
(−) *p53*-exon 5-Me9		CGCGGACG^{Me}CGGGTGCCGGG	5926.9	5926.1
(−) *p53*-exon 5-Me16		CGCGGACGCGGGTGC^{Me}CGGG	5926.9	5926.0

was hydrolyzed to 2′-deoxyribonucleosides with a mixture of deoxyribonuclease I (DNase I, 480 U), phosphodiesterase I (PDE I, 30 mU), and alkaline phosphatase (150 U). N^2-BPDE-dG was isolated by solid-phase extraction (SPE) on C18 Sep-Pak cartridges (Waters Associates, Milford, MA) and further purified by reversed-phase HPLC. The identities of N^2-BPDE-dG and D_8-N^2-BPDE-dG standards were established by MS and UV analysis, as well as by HPLC coelution with an authentic standard of 7*R*,8*S*,9*S*-trihydroxy-10*S*-(N^2-deoxyguanosyl)-7,8,9,10-tetrahydrobenzo[*a*]pyrene. N^2-BPDE-dG and D_8-N^2-BPDE-dG stock solution concentrations were determined by UV spectrophotometry (ϵ_{279} = 40 867).

DNA Purification by HPLC and Purity Control. All DNA oligodeoxynucleotides were purified by HPLC using an Agilent Technologies HPLC system (Model 1100) incorporating a UV diode array detector and a semimicro UV cell. DNA was separated on a Supelcosil LC-18-DB column (4.6 × 150 mm, 5 μm, Supelco, Bellefonte, PA), which was eluted with 100 mM triethylammonium acetate, pH 7 (A) and 25% acetonitrile in 100 mM triethylammonium acetate, pH 7 (B) at a gradient of 25 to 46% B in 40 min, a temperature of 40 °C, and a flow rate of 1 mL/min. The HPLC fractions corresponding to full-length oligodeoxynucleotide products were collected, combined, and thoroughly dried under vacuum to remove most of the ammonium acetate. Impure DNA strands were further purified using the same Supelcosil LC-18-DB column eluted with 150 mM ammonium acetate (A) and acetonitrile (B) at a gradient of 5−12% B in 40 min, at room temperature, and a flow rate of 1 mL/min. DNA amounts were determined by HPLC with UV detection using standard curves constructed from the corresponding unlabeled DNA oligodeoxynucleotides with a Supelcosil LC-18-DB column (2.1 × 250 mm, 5 μm, Supelco, Bellefonte, PA) eluted with 150 mM ammonium acetate (A) and acetonitrile (B) at a gradient of 5−12% B in 40 min. The molecular weight and purity of HPLC-purified DNA were further established by MALDI-TOF MS mass spectrometry using 3-hydroxypicolinic acid as a MALDI matrix. A Bruker Reflex III MALDI-TOF MS instrument (Bruker Daltonics, Billerika, MA) was equipped with a nitrogen laser (Model VSL-337ND, λ = 337 nm, 0.5 ns pulse width) operated at a repetition rate of 3 Hz and an energy of 175 microjoule/pulse. The acceleration energy was 19.9 kV (delayed extraction, delay time = 15 ms). The instrument was operated in linear mode at a laser attenuation of 45−55 and a delay time of 150 ns. Positive ions were detected. The mass range was m/z = 300−18375. The molecular weights of isotopically labeled DNA were within ±0.5 Da of the theoretical values (Table 1). The DNA was considered pure if the impurities peaks in the MALDI-TOF MS spectra and HPLC traces constituted less than 2% of the total area. To obtain double-stranded DNA, we combined equimolar amounts of the two DNA strands in 10 mM Tris buffer, pH 8.0, containing 50 mM NaCl, heated the mixture to 10 °C above the melting temperature, and slowly cooled it to room temperature. The completeness of duplex formation was confirmed by HPLC under nondenaturing conditions.

DNA Treatment with BPDE and Isolation of N^2-BPDE-dG. All experiments were performed in triplicate. Double-stranded DNA (2 nmol) was dissolved in 50 mM Tris-HCl buffer, pH 7.5, to yield a 50 μM concentration. BPDE was dissolved in dry DMSO, and the stock solution concentrations were established by UV spectrophotometry (ϵ_{345} = 48 800). BPDE solution was added to DNA at a specified [BPDE]/[DNA] molar ratio (1:5−5:1), and the reaction mixtures were incubated on ice for 18 h. The final concentration of BPDE was 10−50 μM. The DMSO percentage was kept constant for different treatments and was within 5−10% of the total volume. The reaction mixtures were evaporated to dryness under reduced pressure. BPDE-treated DNA was dissolved in 10 mM Tris-HCl/15 mM $MgCl_2$ buffer, pH 7. Enzymatic digestion of DNA to 2′-deoxyribonucleosides was achieved by incubating with 30 U of DNAse I (12 h at 37 °C), followed by digestion with phosphodiesterase I (60 mU) and alkaline phosphatase (8 U) at pH 9.3 for 18 h. at 37 °C. To confirm the completeness of enzymatic hydrolysis, we

Table 2: Selected Reaction-Monitoring Transitions for Quantitation of BPDE-dG and Related Compounds

N^2-BPDE-dG	*m/z* 570.1(M + H) → *m/z* 454.2 (M-dR + 2H)
[$^{15}N_3$]-N_2-BPDE-dG	*m/z* 573.1(M + H) → *m/z* 457.2 (M-dR + 2H)
[$^{15}N_5$]-N_2-BPDE-dG	*m/z* 575.1(M + H) → *m/z* 459.2 (M-dR + 2H)
D_8-N^2-BPDE-dG (internal standard)	*m/z* 578.1(M + H) → *m/z* 462.2 (M-dR + 2H)

removed small aliquots and analyzed them by HPLC with an Eclipse XDB−C8 column (4.6 × 150 mm, 5 μm, Aglient Technologies) eluted at 1 mL/min. The mobile phase consisted of 150 mM ammonium acetate (A) and acetonitrile (B) eluted at the following gradient: 0−2 min, 0% B; 15 min, 3% B; 18−25 min, 30% B; 28 min, 0%B. UV absorbance at 344 nm (UV maximum for BPDE chromophore) was monitored to ensure that one major adduct peak corresponding to free N^2-BPDE-dG nucleoside is observed. N^2-BPDE-dG was purified by solid-phase extraction using 50 mg C18 SPE cartridges (Waters Associates, Milford, MA). N^2-BPDE-dG eluted in 100% methanol fraction. The SPE fractions containing N^2-BPDE-dG were concentrated under vacuum and analyzed by HPLC-ESI-MS/MS as described below.

HPLC-ESI-MS/MS. A 7000 Finnigan TSQ 7000 mass spectrometer (ThermoQuest, Palo Alto, CA) interfaced with an 1100 Agilent Technologies capillary HPLC system was used for these studies. Chromatographic separation was achieved using a Zorbax SB−C18 column (0.5 × 150 mm, 5 μm, Aglient Technologies) eluted at a flow rate of 15 μL/min. The HPLC solvents were 33% methanol in 15 mM ammonium acetate (A) and 100% acetonitrile (B), and the gradient was 0−30% B in 22.5 min. The mass spectrometer was operated in the positive ion mode. Nitrogen (60−70 psi) was used as a nebulizing and drying gas. Electrospray ionization was typically achieved at a spray voltage of 4.5 kV. The temperature of the heated capillary was 220 °C.

Quantitative analysis of N^2-BPDE-dG was performed via selected reaction monitoring (SRM). The first quadrupole was set to isolate the ions of N^2-BPDE-dG and ^{15}N-N^2-BPDE-dG (*m/z* = 570.2 for ^{14}N-N^2-BPDE-dG, *m/z* = 573.2 for $^{15}N_3$-N^2-BPDE-dG, and *m/z* = 575.2 for $^{15}N_5$-N^2-BPDE-dG, see Table 2). Collision-induced dissociation was performed at the energy of 14 V and Ar gas pressure of 2 mT. The third quadrupole was set to the masses of $(M\text{-}dR + 2H)^+$ (*m/z* = 454.1.2 for [^{14}N]-N^2-BPDE-dG, *m/z* = 457.1 for $^{15}N_3$-N^2-BPDE-dG, and *m/z* = 459.1 for $^{15}N_5$-N^2-BPDE-dG, see Table 2). For dose−response experiments involving D_8-N^2-BPDE-dG internal standard, the analogous SRM transition *m/z* 578.2 (M + H) → *m/z* 462.1 was used. The scan time was 1 s, and the isolation width was 0.7 amu. The instrument was tuned to maximum sensitivity during direct infusion of N^2-BPDE-dG standards.

The extent of N^2-BPDE-dG formation at the $^{15}N_5$-labeled guanine (X) was calculated from the following equation:

$$\%\ \text{reaction at X} = A_{\text{BPDE-dX}}/(A_{\text{BPDE-dX}} + A_{\text{BPDE-dG}})$$

where $A_{\text{BPDE-dG}}$ and $A_{\text{BPDE-dX}}$ are the areas under the HPLC-ESI-MS/MS peaks corresponding to unlabeled and [^{15}N]-labeled adducts, respectively.

Quantitative analyses of N^2-BPDE-dG in dose−response samples using unlabeled DNA were based on the ratio of the area under the peaks corresponding to the analyte and the D_8 internal standard:

$$Q_{\text{an}} = A_{\text{an}}/A_{\text{is}} \times Q_{\text{is}}$$

where Q_{an} and Q_{is} are the amounts of the analyte and the internal standard; A_{an} and A_{is} are the areas under the peaks corresponding to the analyte and the internal standard, respectively. The linearity was checked using calibration curves constructed by spiking known amounts of the analyte with the internal standard.

Scheme 1: Strategy for Quantitation of BPDE-dG Adducts at Specific Sites within DNA Sequence

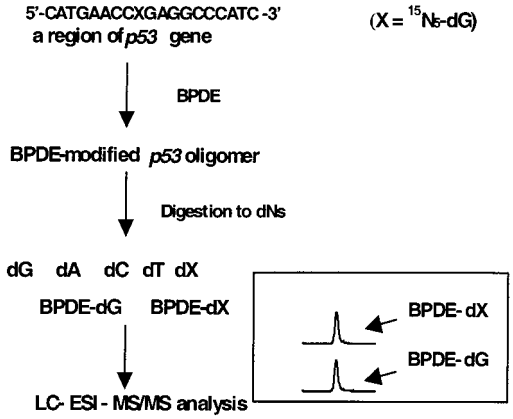

Statistical Analyses of the Data. All statistical analyses have been performed by Susan Schulte at the Biostatistics Core of the University of Minnesota Cancer Center with the ANOVA model. The reactivity of individual guanines were compared by t-test using the formula $(\mu_1 - \mu_2)/(\text{MSE}\cdot(1/n_2 + 1/n_2))^{1/2}$, where μ's are the mean reactivities at positions 1 and 2, respectively, and MSE is the mean squared error from ANOVA. To compare the reactivity at specified guanine nucleobase with the theoretical "random" reactivity value, we used the following formula $(\mu_i - c)/(\text{MSE}(1/n_i))^{1/2}$, where μ_i is the mean reactivity at position *i*, *c* is the theoretical reactivity value, and MSE is the mean squared error from ANOVA.

RESULTS

Stable Isotope Labeling HPLC-ESI-MS/MS. This investigation has focused on quantifying BPDE-induced lesions at specific guanine nucleobases within mutation-prone regions of the *K-ras* and *p53* gene using stable isotope labeling. Stable isotope labeling is commonly used in mass spectrometry of chemically modified DNA nucleosides, e.g., in isotope dilution methods where the isotope-labeled analogue serves as an internal standard for quantitation (*31*−*33*). These methods provide accurate values for the total amounts of DNA lesions but do not distinguish between adducts produced at the mutational hot spots of critical genes and those originating from less frequently mutated DNA regions. Our approach is based on placing ^{15}N-labeled guanine nucleobases at specific positions within DNA oligodeoxynucleotides representing gene sequences of interest, followed by BPDE treatment, enzymatic hydrolysis, and HPLC-ESI-MS/MS analysis of the nucleoside adducts (Scheme 1). The BPDE adducts formed at the ^{15}N-labeled guanine can be distinguished from the lesions originating at other sites by

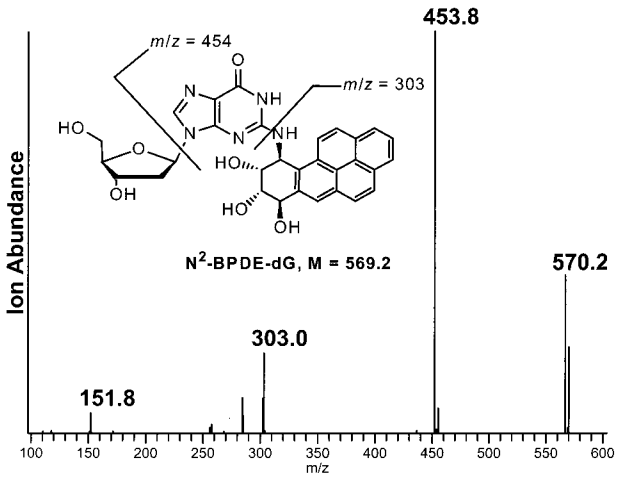

FIGURE 1: ESI$^+$ MS/MS spectrum of N^2-BPDE-dG. Finnigan MAT TSQ 7000 (ThermoQuest, San Jose, CA) was operated in the ESI$^+$ mode (spray voltage, 5 kV; collision gas pressure, 2 mT; collision energy, 14 V; heated capillary, 220 °C; electron multiplier, 2200 V). N^2-BPDE-dG (2 μM in 1:1 methanol/water) was infused at a flow rate of 5 μL/min.

their molecular weight, which is increased due to the presence of ^{15}N atoms in the molecule (Figure 2). We used dG phosphoramidites containing either three or five ^{15}N atoms with no change in experimental results. However, the contribution of naturally occurring isotopes (e.g., ^{13}C), requires that the labeled dG differs from the normal dG by at least two mass units. By preparing several oligomers of the same sequence but with different labeled positions (Table 1), we can determine the extent of adduct formation at each site of interest (Scheme 1). HPLC-ESI-MS/MS quantitation of N^2-BPDE-dG is based on the facile loss of deoxyribose ($M = 116$) from the molecular ion of the adduct ($m/z = 570.2$, M + H) under collision induced dissociation conditions, leading to the predominant fragment at $m/z = 454.1$ (Figure 1, Table 2). ^{15}N-labeled N^2-BPDE-dG gives rise to analogous molecular and fragment ions whose m/z values are increased by the number of ^{15}N atoms in the molecule (Table 2). The extent of adduct formation at the isotopically labeled nucleobase is calculated directly from the ratios of the areas under the HPLC-ESI MS/MS peaks corresponding to ^{15}N and unlabeled adducts, respectively (Figure 2).

Our stable isotope labeling approach (Scheme 1) requires that the LC-ESI-MS/MS sensitivity is sufficient to detect BPDE-induced DNA adducts formed at a specific guanine nucleobase within a DNA sequence. For example, to study the formation of N^2-BPDE-dG at a single G within a DNA sequence containing 20 guanines, the sensitivity must be 20-fold greater than for a "normal" HPLC-ESI-MS/MS assay measuring the sum of all N^2-BPDE-dG adducts. Our approach uses capillary HPLC at a flow rate of 15 μL/min (See Experimental Part for details). The use of capillary LC enables at least a 10× increase in sensitivity relative to typical 1 mm columns eluted at a flow rate of 60−70 μL/min (*34*), resulting in detection limits in the low fmol region (20 fmol for N^2-BPDE-dG at S/N = 3). Figure 3 shows a typical calibration curve for the LC-ESI-MS/MS analysis of BPDE-dG using D_8-N^2-BPDE-dG (M + H = 578) as an internal standard. The calibration curves were linear from 0.07 to 2200 pmol N^2-BPDE-dG (Figure 3).

In the first part of this investigation, we sought to establish DNA amounts and BPDE exposure conditions that give rise to a sufficient number of N^2-BPDE-dG adducts to enable the detection of the lesions originating from specific guanine nucleobase. Double-stranded DNA oligomers (2 nmol) were treated with BPDE at varying molar ratios [BPDE]:[DNA] = 1:5, 1:1, and 5:1. All treatments were performed in triplicate. The overall level of BPDE modification calculated from HPLC peak area ratios of BPDE-modified and unmodified DNA were within the range of 0.5−1.6%, indicating that no more than one adduct per DNA molecule was formed ("single hit" conditions). The amounts of N^2-BPDE-dG ranged from 5 to 50 pmol/nmol dG, depending on exposure concentration (Figure 4). We therefore concluded that a 2 nmol DNA sample per exposure was sufficient for our purposes.

Quantitative enzymatic digestion of BPDE-modified DNA to 2′-deoxyribonucleosides is necessary to enable the quantitative analysis of N^2-BPDE-dG adduct formed at specific guanines within DNA sequences. We and others have noted the ability of N^2-BPDE-dG adducts to block phosphodiesterase enzymes, which may lead to incomplete digestion of BPDE-modified DNA (*30*, *35*, *36*). However, our earlier experiments also indicated that N^2-BPDE-dG-containing DNA can be completely hydrolyzed by extensive incubation with an excess of phosphodiesterase (*35*). We have varied incubation times, enzyme amounts, and buffer pH/composition in order to identify enzymatic digestion conditions resulting in quantitative hydrolysis of BPDE-treated DNA. The digests were examined by HPLC with UV detection at 279 and 344 nm (absorption maxima for BPDE-dG adducts) and 260 nm (to detect of dG, dT, dA, and dC). If the digestion is complete, the only BPDE-dG adduct peak observed should correspond to free N^2-BPDE-dG deoxyribonucleoside. Furthermore, the molar amounts of released unmodified nucleosides should be consistent with the number of nucleobases of each type in the sequence. The digests that appeared complete by HPLC-UV analysis were further analyzed by HPLC-ESI-MS/MS. The best results were achieved when BPDE treated DNA was first incubated with DNase in 10 mM Tris-HCl/15 mM $MgCl_2$, pH 7. Following 12−14 h incubation, the pH was adjusted to 9.3 with Tris-HCl (final concentration of Tris = 50 mM), and the samples were digested with a mixture of PDE I and alkaline phosphate for 18−22 h. The digestions were considered complete since no increase of N^2-BPDE-dG amounts was observed upon adding fresh enzyme and additional digestion times. We have noted that the presence of low EDTA concentrations in the digestion buffer inhibited DNA hydrolysis, probably by scavenging the magnesium ions required for phosphodiesterase I activity. EDTA was thus excluded from our experiments.

Distribution of N^2-BPDE-dG Adducts within K-ras Gene Derived DNA Sequence Containing Codon 12. K-ras codon 12 is the major hot spot for G → T transversions in smoking-induced lung adenocarcinoma (*7*−*12*). Primer extension and site specific mutagenesis of N^2-BPDE-dG gives rise to primarily G → T transversions (*4*−*6*, *37*), suggesting that the *K-ras* mutations observed in lung tumors of smokers may be due to the exposure to benzo[*a*]pyrene in tobacco smoke. Alternatively, other tobacco carcinogens, e.g., tobacco specific nitrosamine 4-(methylnitrosamino)-1-(3-pyridyl)-1-

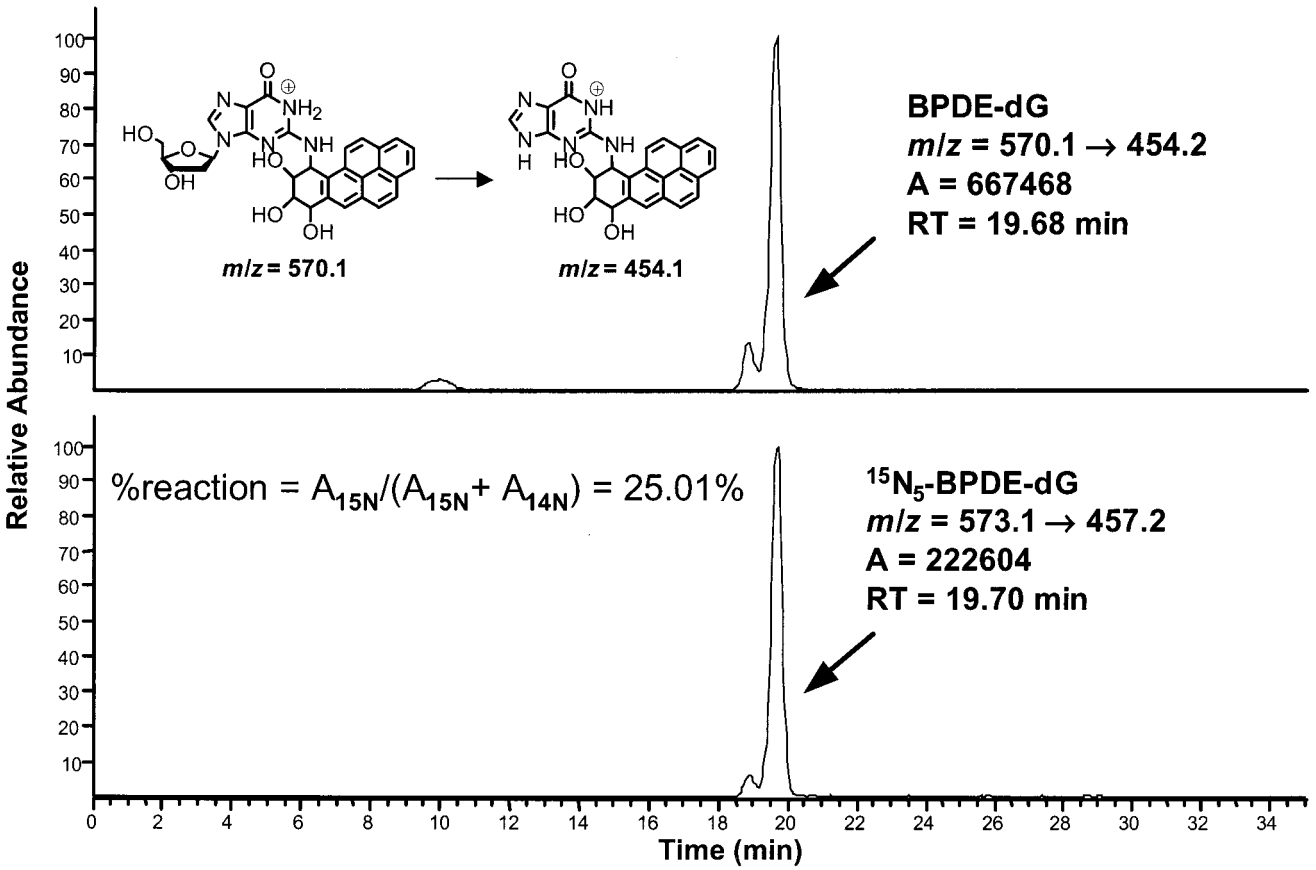

FIGURE 2: HPLC-ESI-MS/MS analysis of N^2-BPDE-dG in [$^{15}N_3$]-labeled *K-ras* derived DNA fragment, CCC GGC ACC ^{Me}CXC GTC CGC G (X = [$^{15}N_3$-dG]). Selected reaction monitoring was performed using the transitions: BPDE-dG, *m/z* 570.1 → *m/z* 454.0; [$^{15}N_3$]-BPDE-dG, *m/z* 573.1 → *m/z* 457.0. HPLC: Aglient 1100 series capillary liquid chromatograph (Agilent technologies). A Zorbax SB-C18 column (150 × 0.5 mm, 5 μm, Agilent Technologies) was eluted at a flow rate of 15 μL/min. HPLC solvents: A = 33% methanol in 15 mM ammonium acetate, B = acetonitrile, gradient 0−30% B in 22.5 min. MS: Finnigan MAT TSQ 7000 (ThermoQuest, San Jose, CA) operated in ESI$^+$ mode. Spray voltage, 5 kV; collision gas pressure, 2 mT; heated capillary, 200 °C; electron multiplier, 2200 V.

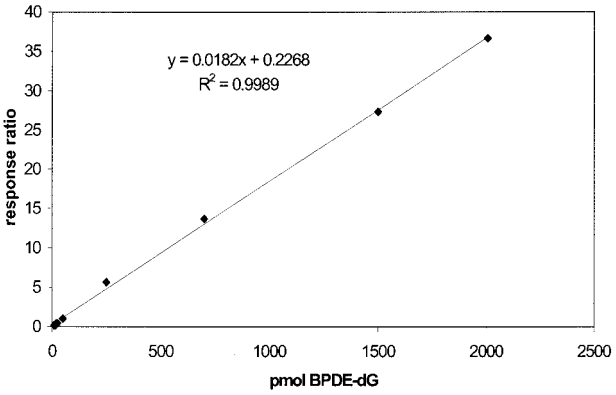

FIGURE 3: Calibration curve for LC-ESI-MS/MS analysis of N^2-BPDE-dG with D_8-BPDE-dG as an internal standard. See Figure 2 for HPLC-ESI MS/MS conditions.

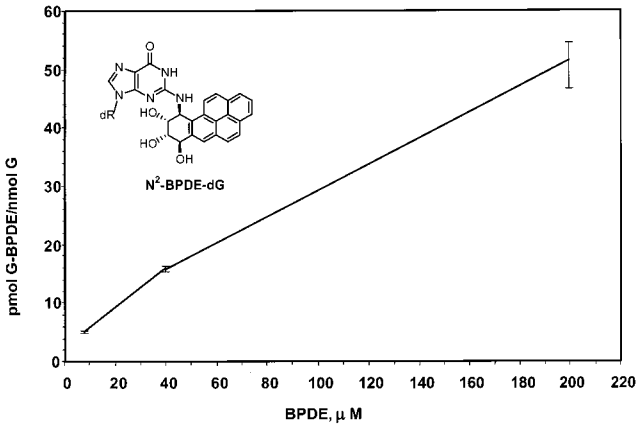

FIGURE 4: Formation of N^2-BPDE-dG in BPDE treated *K-ras* double-stranded oligodeoxynucleotide derived from *K-ras* exon 1: GGA GCT GGT GGC GTA GGC.

butanone (NNK) or reactive oxygen species, may cause these genetic changes. We examined the formation of N^2-BPDE-dG adducts at specific guanine nucleobases within a DNA sequence containing *K-ras* codons 10−15. A series of synthetic oligodeoxynucleotides 5′-$G_1G_2A\mathbf{G_3}CT\mathbf{G_4G_5}T\mathbf{G_6}G_7$-CGT AGGC-3′ (codon 12 = $\mathbf{G_4G_5}$T) were prepared, each containing a single ^{15}N-guanine at positions $\mathbf{G_3}$, $\mathbf{G_4}$, $\mathbf{G_5}$, or $\mathbf{G_6}$ (Table 1). The extent of N^2-BPDE-dG formation at each guanine was quantitated by HPLC-ESI-MS/MS as described above.

Since the double-stranded *K-ras* 19-mer contains a total of 13 guanines, the theoretical amount of N^2-BPDE-dG adducts formed at each guanine in the absence of any sequence effects is 100%/13 = 7.7%. We found that the formation of N^2-BPDE-dG within the *K-ras*-derived sequence was not uniform. As much as 16.9% of N^2-BPDE-dG adducts were formed at $\mathbf{G_4}$, 8−10% were produced at $\mathbf{G_5}$ and $\mathbf{G_6}$, and only 3.5% of the lesions originated from $\mathbf{G_3}$ (Figure 5a). Statistical analysis indicates that the reactivities

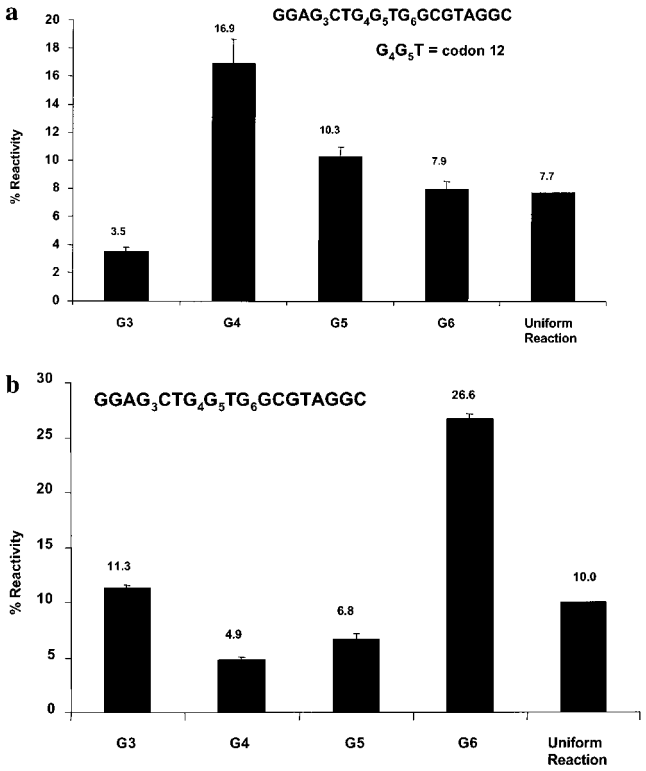

FIGURE 5: Relative formation of N^2-BPDE-dG at guanine nucleobases within double stranded (a) and single stranded (b) *K-ras* gene sequence: $G_1G_2A\ G_3CTG_4G_5TG_6G_7C\ G_8TA\ G_{10}GC$ (codon 12 = G_4G_5T). The data were compiled from two separate experiments ($N = 3-6$). The percent of reaction at each guanine was calculated from the area ratio of ^{15}N-labeled HPLC-ESI-MS/MS peak to the sum of unlabeled and ^{15}N-labeled adduct peak areas. The random reaction value was determined from the total number of guanine nucleobases in both DNA strands.

of $\mathbf{G_4}$ and $\mathbf{G_5}$ are significantly above the theoretical value ($P < 0.001$), while $\mathbf{G_3}$ gives rise to lower than average number of adducts ($P < 0.001$). The percent reaction at $\mathbf{G_6}$ (7.9%) is within the theoretical value ($P > 0.5$). These results indicate that in double stranded DNA, N^2-BPDE-dG forms preferentially at the first guanine of *K-ras* codon 12, the major hotspot for activating G → T transversions in smoking-induced lung adenocarcinoma (*7*−*10*). This evidence, together with the observations that G →T transversions are the major type of mutations resulting from N^2-BPDE-dG (*4*−*6*), is consistent with the involvement of BPDE or analogous PAH metabolites in the induction of *K-ras* gene mutations in smokers, although the contribution of other tobacco carcinogens cannot be excluded.

When the experiments were repeated with single-stranded DNA, a very different pattern of reactivity was observed (Figure 5b). In contrast with our results for the double stranded *K-ras* sequence, the guanines of single-stranded codon 12 ($\mathbf{G_4}$ and $\mathbf{G_5}$) exhibit low reactivity toward BPDE (4−5%), while the neighboring guanines ($\mathbf{G_3}$ and $\mathbf{G_6}$) are more reactive, accounting for 12−26% of the total adduct formation (Figure 5b). The presence of distinct sequence preferences for BPDE reactions with single-stranded DNA may be due to the local secondary structures in the *K-ras* oligodeoxyribonucleotide. Such secondary structures are common for DNA fragments containing multiple guanines. In addition, sequence-dependent noncovalent binding of

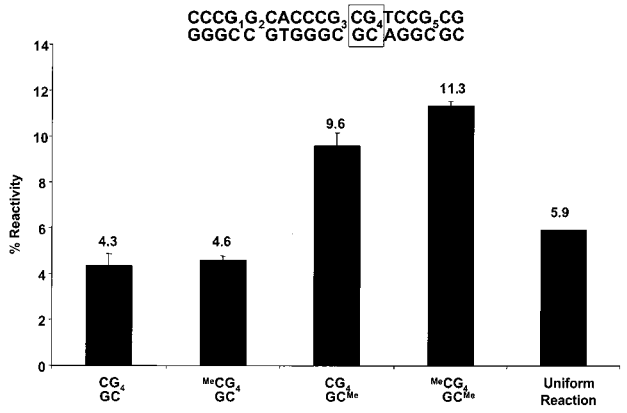

FIGURE 6: Effect of cytosine methylation on the extent of N^2-BPDE-dG formation (%) at *p53* codon 157 (G_4TC) in double-stranded oligodeoxynucleotide derived from *p53* exon 5*:* CCG_1G_2-$CACCCG_3CG_4TCCG_5CG$. The data were compiled from two separate experiments ($N = 4-6$). The relative adduct formation at each guanine was calculated from the HPLC-ESI-MS/MS area ratio of ^{15}N-labeled peak to the sum of unlabeled and ^{15}N-labeled adduct peak areas. The random reaction value was determined from the total number of guanine nucleobases in both DNA strands.

BPDE to different positions in single-stranded DNA may play a role (*38*).

Effect of Cytosine Methylation on the Formation of N^2-BPDE-dG Adducts within the p53 Gene Sequence. Endogenous methylation of cytosine is involved in gene regulation and possibly in cancer (*39*). Sixty to eighty percent of CpG sites in the human genome contain 5-methylcytosine, including all CpG sites along exons 5−8 of the *p53* tumor suppressor gene (*40*). Cytosine methylation within CpG dinucleotides has been shown to stimulate guanine reactions with carcinogens and drugs, e.g., mitomycin C(*41*), esperamicins (*42*), and BPDE (*43*), while guanine modifications with *N*-methyl-*N*-nitrosourea and bleomycin are inhibited by the neighboring 5-Me-C (*44*−*46*). BPDE-induced DNA damage at guanine nucleobases within CpG context has been shown to be significantly enhanced by cytosine methylation (*26*, *43*, *47*, *48*). However, questions remain regarding the mechanism of this effect, especially since CpG dinucleotides contain two 5-Me-C nucleobases (one in each DNA strand), both of which may influence the reactivity of target guanine toward BPDE.

To examine the effects of the 5′ neighboring 5-Me-C and the base paired 5-Me-C on N^2-BPDE-dG formation independently, we placed methylated cytosine in either one or both DNA strands of the *p53* codon 157 dinucleotide (Cp$\mathbf{G_4}$, Table 1). Isotopic labeling HPLC-ESI-MS/MS analysis of N^2-BPDE-dG formation in these oligodeoxynucleotides indicated that the reactivity of $\mathbf{G_4}$ toward BPDE was indeed affected by the methylation state of the neighboring cytosines (Figure 6). In the absence of cytosine methylation, the amount of N^2-BPDE-dG formed at $\mathbf{G_4}$ was within the range expected for a uniform reaction ($P > 0.07$), indicating the lack of sequence specificity (Figure 6). The introduction of 5-Me-dC within Cp$\mathbf{G_4}$ dinucleotide of the same DNA strand did not significantly increase the extent of N^2-BPDE-dG formation at $\mathbf{G_4}$ ($P > 0.5$). On the contrary, a large increase in N^2-BPDE-dG adduct formation (from 4.3 to 9.6%) was observed when 5-Me-dC was placed in the opposite strand from the target G ($P < 0.001$, Figure 6). The highest yield of N^2-BPDE-dG (11.3%) was observed when both the 5′

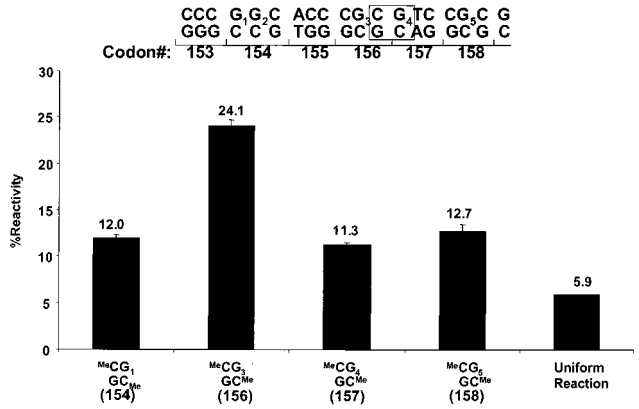

FIGURE 7: Relative formation of N^2-BPDE-dG at guanine nucleobases within a double-stranded oligodeoxynucleotide representing a region *p53* exon 5 containing frequently mutated codons 157 and 158*:* $CCG_1G_2CACCCG_3CG_4TCCG_5CG$). The data were compiled from two separate experiments ($N = 3-6$). The relative adduct formation at each guanine was calculated from the area ratio of HPLC-ESI-MS/MS peak corresponding to [^{15}N]-N^2-BPDE-dG to the sum of unlabeled and [^{15}N]-adduct peak areas. The random reaction value was determined from the total number of guanine nucleobases in both DNA strands.

neighboring and the base-paired cytosine were methylated (Figure 6). While the total increase in target guanine reactivity toward BPDE can be explained by the additive effect of the 5-methylcytosines located 5′ and across from the target guanine nucleobase, methylation of the base paired cytosine appears to have a greater effect on N^2-BPDE-dG adduct formation (Figure 6).

Distribution of N^2-BPDE-dG Adducts within the p53-Derived DNA Sequence Containing Codon 158. Our rationale for selecting exon 5 of *p53* tumor-suppressor gene for these studies is based on the fact that this region of *p53* contains the mutational "hotspot" characteristic for lung cancer (codons 157 and 158) (*19*). Other major *p53* mutational hotspots (codons 245, 249, and 273) are commonly seen in other tumor types (*19*) and may be a result of mutant selection for growth rather than originate from tobacco carcinogen-induced DNA damage (*49*). On the other hand, codon 157 and 158 mutations are more specific for lung cancer of smokers (*19*).

To compare the reactivity of different guanines within *p53* exon 5 toward BPDE, we prepared synthetic oligodeoxynucleotides $CC\mathbf{G_1}G_2CACCC\mathbf{G_3}C\mathbf{G_4}$ $TCC\mathbf{G_5}CG_6$ containing [^{15}N] label at one of the highlighted positions, $\mathbf{G_1}$, $\mathbf{G_3}$, $\mathbf{G_4}$, or $\mathbf{G_5}$ (codon 157 = G_4TC, codon 158 = CG_5C). Cytosine nucleobases were replaced with 5-Me-C in accordance with the patterns of endogenous cytosine methylation within CpG dinucleotides of the *p53* gene (*40*). All four methylated positions $\mathbf{G_1}$, $\mathbf{G_3}$, $\mathbf{G_4}$, and $\mathbf{G_5}$ exhibited higher-than-average reactivity toward BPDE ($P < 0.005$). The yields of N^2-BPDE-dG adducts followed the following order: **G3** (codon 156) $\gg$ **G5** (codon 158) $>$ $\mathbf{G_1}$ (codon 154) $\cong$ $\mathbf{G_4}$ (codon 157) (Figure 7). These results are remarkably similar to the data of Pfeifer et al., who used LMPCR of UvrABC-cleaved DNA to visualize the sites of BPDE reaction within *p53* gene sequence (*25*, *43*). However, this pattern of reactivity does not correlate with G → T transitions in lung cancer carcinoma, where genetic changes are much more prevalent at codons 157 and 158 than at codons 154 and 156 (*14*, *22*−*24*).

DISCUSSION

Although it is widely accepted that exposure to carcinogens in tobacco smoke gives rise to DNA adducts that in turn can contribute to the initiation of lung cancer, the exact link between DNA adduction and lung cancer in smokers has not been established. The presence of characteristic hot spots for mutations in smoking-induced lung tumors can result from sequence-selective DNA adduct formation, sequence effects on repair rates, context-dependent misincorporation during cell replication, or mutant selection for growth. The effects of sequence context on mispairing capacity and repair can be studied by site specific mutagenesis (*50*). However, methods capable of determining the extent of adduct formation at specific positions within gene sequences are lacking. Indirect approaches, e.g., ligation-mediated PCR of the DNA fragments generated by endonuclease or hot piperidine treatment (*28*, *51*, *52*), do not analyze DNA adducts per se but, rather, detect DNA nicks produced at the sites of nucleobase modifications. The cleavage step itself may be sequence-dependent, leading to possible errors in quantitation. Furthermore, since the structural identities of the lesions cannot be determined, the usefulness of LMPCR and related techniques for mapping specific DNA damage resulting from an exposure to a mixture of carcinogens (e.g., cigarette smoke or any in vivo exposure) is limited.

In the present report, we describe a mass spectrometry-based approach that can directly quantify the formation of carcinogen-DNA lesions at specific positions within DNA sequences. The formation of DNA adducts at specific nucleobases is monitored by introducing stable isotope-labeled nucleobase at a specific site within a DNA sequence, followed by carcinogen treatment and analysis of the resulting adducts by liquid chromatography-electrospray ionization mass spectrometry (HPLC-ESI-MS/MS). Since the presence of ^{15}N isotope in guanine molecule should not affect its reactions with electrophiles, adduct yields at the ^{15}N-labeled position represent the extent of reaction at this site in unlabeled DNA. The use of short DNA sequences as models for nuclear DNA in our study is justified by the evidence that chromatin structure has little effect on the distribution of DNA damage induced by BPDE and methylating agents (*25*, *43*, *51*). The stable isotope labeling HPLC-MS approach should be applicable to a large range of DNA modifications from simple alkylating agents to drug-induced lesions. For example, adducts that cannot be converted to strand breaks for PAGE analysis (e.g., O^6-modified guanines) can be readily quantitated and chemically identified from their molecular weights. Although the stable isotope-labeling HPLC-ESI-MS/MS approach is currently limited to model systems (synthetic DNA), studies are planned to expand the applicability of this methodology to cell culture experiments.

The present investigation has focused on the patterns of DNA modification with proposed causative agent for smoking-induced lung cancer, BPDE. We selected DNA sequences representing mutation-prone regions of the two critical genes for lung cancer, *p53* tumor suppressor gene and *K-ras* protooncogene. The region of *K-ras* gene selected for this study contains codon 12 frequently mutated in lung tumors of smokers (*10*, *18*). The *p*53 region containing codons 157 and 158 of the exon 5 was selected on the basis of the specificity of this mutational hot spot for lung cancer (*19*).

A large variation (~5-fold) in BPDE binding to the N^2 position of different guanines was observed for both sequences. Previous reports have documented the influence of neighboring nucleobases on N^2-BPDE-dG adduct formation (*47*, *53*, *54*). For example, guanine nucleobases surrounded by pyrimidines have been found more reactive toward BPDE than those surrounded by purines (*53*). Our investigation reveals a more complex relationship between DNA sequence and reactivity toward BPDE, which cannot be explained simply by the neighboring nucleobases. For example, G4 and G6 nucleobases of the *K-ras* sequence have the same T*G*G sequence context but give rise to a different number of N^2-BPDE-dG adducts (Figure 5a), suggesting that more distant nucleobases have an effect on reactivity of the target G. This also suggests that the results of model studies that employ synthetic oligomers with a single G in a varied sequence context are not always applicable to actual gene-derived sequences where multiple guanines compete to reactions with electrophiles.

Our results support previous reports on the stimulating effect of cytosine methylation on N^2-BPDE-dG formation within CpG sequences (*43*). In theory, the increased N^2-BPDE-dG formation at methylated sites may be due to the increased BPDE prestacking prior to nucleophilic attack (*38*), local helical unwinding, or increased nucleophilicity of guanine as a result of electron-donating effect of the 5-methyl group transmitted through the 5-Me-C·G base pair (*41*). Our experiments reveal a 2.5-fold increase of N^2-BPDE-dG yields due to the base paired 5-Me-C, while methylation of the 5′-neighboring cytosine had little effect on reactivity (Figure 6). These results can be explained either by the electronic effect of the 5-Me-C methyl group transmitted through hydrogen bonds (*41*) or by the increased formation of precovalent intercalative complexes at the 5-Me-C·G sites (*38*). Weisenberger et al. (*48*) have detected structural changes in DNA duplexes containing both 5-Me-C and N^2-BPDE-dG adduct. It is possible that hydrophobic interactions between BPDE and the 5-Me-C nucleobase across from the target G could lead to a lowered transition state energy for nucleophilic attack of the N^2 amino group of the guanine at the C-10 position of BPDE.

Our data are in contrast with the report of Pradhan et al. (*47*), who observed increased adduct yields due to 5-Me-C within the same strand as the target G and no effect of the hydrogen-bonded 5-Me-C on guanine reactivity toward BPDE. These discrepancies may be due to differences in analytical approaches, treatment conditions, or simply the choice of DNA sequences. For example, unlike DNA used in previous studies, our ODN sequences are derived from actual genes and contain multiple guanine nucleobases that are potential targets for BPDE reactions. Interestingly, we did observe a 50% increase in N^2-BPDE-dG yield when methylated cytosine was introduced 5′ from the target G of a single-stranded oligonucleotide (results not shown). This effect, however, was not observed with a double-stranded version of the same DNA (Figure 6).

The distribution of N^2-BPDE-dG lesions within the double-stranded DNA sequence derived from the *K-ras* gene exhibited a good correlation with the pattern of *K-ras* mutations observed in lung cancer (Figure 5a). The first guanine of *K-ras* codon 12 (GGT) is frequently mutated to thymine (TGT) in tumor DNA, leading to the activation of the *K-ras* protooncogene (*7*−*12*). The same guanine (G4 in our numbering system) was found to give rise to the highest number of N^2-BPDE-dG adducts within the *K-ras* oligodeoxynucleotide (Figure 5a). These data are consistent with the involvement of benzo[*a*]pyrene or other tobacco PAHs in the induction of *K-ras* gene mutations observed in lung cancer. However, DNA damage induced by other tobacco carcinogens, e.g., *N*-nitrosamines, 1,3-butadiene, and reactive oxygen species, may also contribute to these mutations. The final proof of this relationship awaits the in vivo mapping of both N^2-BPDE-dG lesions and mutations within *K-ras* and *p53* genes. As in the case with the *p53* sequence, the distribution of damage in single stranded DNA was completely different (Figure 5b) and, unsurprisingly, did not correlate with mutations.

Multiple guanines within *p53* exon 5, including guanine nucleobases within codons 154, 156, 157, and 158, exhibit an increased reactivity toward BPDE (Figure 7). This distribution of BPDE-induced damage is consistent with the data of Denissenko et al. obtained by *uvr*ABC incision assay (*25*, *43*). Since methods of detecting BPDE lesions applied by the two laboratories are totally different, this validates the use of both approaches for mapping BPDE-induced damage. Each approach has its advantages: while isotopic labeling-LC-MS is quantitative, applicable to a wide range of lesions, and provides adduct identity information, LMPCR PAGE can be used for DNA samples from biological sources and provides information over wider gene regions. A direct comparison of the distribution of BPDE-induced lesions with the patterns of mutations observed in lung tumors reveals a lack of correlation between N^2-BPDE-dG formation and *p53* exon 5 mutations. For example, the yields of N^2-BPDE-dG at codons 156 and 154 are higher than those at the prominent mutational hot spots, codons 157 and 158. This may be due to the effect of sequence context on the rates of repair and/or mispairing efficiency of N^2-BPDE-dG, mutant selection for growth, or simply due to a different origin of these genetic changes. Other tobacco carcinogens, such as tobacco specific nitrosamines (e.g., NNK), aromatic amines, or reactive oxygen species, may target these sites within the *p53* gene, giving rise to initiating mutations for lung cancer (*1*). Studies are in progress at our laboratory to establish the distribution of NNK-induced DNA damage within DNA sequences derived from *p53* and *K-ras* gene.

ACKNOWLEDGMENT

We thank Prof. Stephen Hecht (MIT) for providing D_8-BPDE and for the helpful discussions, Dr. Peter Villalta for his assistance with the TSQ mass spectrometer, Agilent Technologies for providing the 1100 Capillary HPLC system, and Prof. Nicholas Geacintov (New York University) for detailed comments and suggestions on the manuscript.

REFERENCES

1. Hecht, S. S. (2000) *J. Natl. Cancer Inst. 92*, 782−783.
2. IARC (1983) *Monographs on the Evaluation of the Carcinogenic Risk of Chemicals to Humans: Polycyclic Aromatic Compounds, Part I, Chemical, Environmental, and Experimental Data*, Vol. 32, Intenational Agency for Research on Cancer., Lyon, France.
3. Osborne, M. R., Beland, F. A., Harvey, R. G., and Brookes, P. (1976) *Int. J. Cancer 18*, 362−368.
4. Mackay, W., Benasutti, M., Drouin, E., and Loechler, E. L. (1992) *Carcinogenesis 13*, 1415−1425.

5. Jelinsky, S. A., Liu, T., Geacintov, N. E., and Loechler, E. L. (1995) *Biochemistry 34*, 13545−13553.
6. Zhang, Y., Yuan, F., Wu, X., Rechkoblit, O., Taylor, J. S., Geacintov, N. E., and Wang, Z. (2000) *Nucleic Acids Res. 28*, 4717−4724.
7. Slebos, R. J., and Rodenhuis, S. (1992) *J. Natl. Cancer Inst. Monogr*. 23−29.
8. Westra, W. H., Slebos, R. J., Offerhaus, G. J., Goodman, S. N., Evers, S. G., Kensler, T. W., Askin, F. B., Rodenhuis, S., and Hruban, R. H. (1993) *Cancer 72*, 432−438.
9. Siegfried, J. M., Gillespie, A. T., Mera, R., Casey, T. J., Keohavong, P., Testa, J. R., and Hunt, J. D. (1997) *Cancer Epidemiol. Biomarkers Prev. 6*, 841−847.
10. Westra, W. H., Baas, I. O., Hruban, R. H., Askin, F. B., Wilson, K., Offerhaus, G. J., and Slebos, R. J. (1996) *Cancer Res. 56*, 2224−2228.
11. Rodenhuis, S., and Slebos, R. J. (1992) *Cancer Res. 52*, 2665s-2669s.
12. Slebos, R. J., Hruban, R. H., Dalesio, O., Mooi, W. J., Offerhaus, G. J., and Rodenhuis, S. (1991) *J. Natl. Cancer Inst. 83*, 1024−1027.
13. Slebos, R. J., Baas, I. O., Clement, M. J., Offerhaus, G. J., Askin, F. B., Hruban, R. H., and Westra, W. H. (1998) *Hum. Pathol. 29*, 801−808.
14. Hussain, S. P., and Harris, C. C. (1999) *Mutat. Res. 428*, 23−32.
15. Harris, C. C. (1996) *J. Natl. Cancer Inst. 88*, 1442−1455.
16. Hussain, S. P., Hollstein, M. H., and Harris, C. C. (2000) *Ann. N.Y. Acad. Sci. 919*, 79−85.
17. Husgafvel-Pursiainen, K., Boffetta, P., Kannio, A., Nyberg, F., Pershagen, G., Mukeria, A., Constantinescu, V., Fortes, C., and Benhamou, S. (2000) *Cancer Res. 60*, 2906−2911.
18. Rodenhuis, S., Slebos, R. J., Boot, A. J., Evers, S. G., Mooi, W. J., Wagenaar, S. S., van Bodegom, P. C., and Bos, J. L. (1988) *Cancer Res. 48*, 5738−5741.
19. Hainaut, P., and Pfeifer, G. P. (2001) *Carcinogenesis 22*, 367−374.
20. Belinsky, S. A., Swafford, D. S., Finch, G. L., Mitchell, C. E., Kelly, G., Hahn, F. F., Anderson, M. W., and Nikula, K. J. (1997) *Environ. Health Perspect. 105 Suppl. 4*, 901−906.
21. Bennett, W. P., Hussain, S. P., Vahakangas, K. H., Khan, M. A., Shields, P. G., and Harris, C. C. (1999) *J. Pathol. 187*, 8−18.
22. Hussain, S. P., and Harris, C. C. (2000) *Mutat. Res. 462*, 311−322.
23. Hussain, S. P., Amstad, P., Raja, K., Sawyer, M., Hofseth, L., Shields, P. G., Hewer, A., Phillips, D. H., Ryberg, D., Haugen, A., and Harris, C. C. (2001) *Cancer Res. 61*, 6350−6355.
24. Pfeifer, G. P. (2000) *Mutat. Res. 450*, 155−166.
25. Denissenko, M. F., Pao, A., Tang, M., and Pfeifer, G. P. (1996) *Science 274*, 430−432.
26. Pfeifer, G. P., Tang, M., and Denissenko, M. F. (2000) *Curr. Top. Microbiol. Immunol. 249*, 1−19.
27. Tang, M.-S., Feng, Z., Hu, W., Chen, J., Li, H., Rom, W., Pao, A., and Hung, M.-C. (2001) Carcinogen-DNA Adducts Are Preferentially Formed and Poorly Repaired at Codon 12 of the K-ras Gene, a Mutation Hotspot in Lung Cancers of Cigarette Smokers, *Proc. Am. Assoc. Cancer Res. 42*, 694.
28. Tang, M. S., Zheng, J. B., Denissenko, M. F., Pfeifer, G. P., and Zheng, Y. (1999) *Carcinogenesis 20*, 1085−1089.
29. McGregor, W. G., Wei, D., Chen, R. H., Maher, V. M., and McCormick, J. J. (1997) *Mutat. Res. 376*, 143−152.
30. Barry, J. P., Norwood, C., and Vouros, P. (1996) *Anal. Chem. 68*, 1432−1438.
31. Frelon, S., Douki, T., Ravanat, J. L., Pouget, J. P., Tornabene, C., and Cadet, J. (2000) *Chem. Res. Toxicol. 13*, 1002−1010.
32. Tretyakova, N. Y., Chiang, S. Y., Walker, V. E., and Swenberg, J. A. (1998) *J. Mass Spectrom. 33*, 363−376.
33. Knize, M. G., Kulp, K. S., Malfatti, M. A., Salmon, C. P., and Felton, J. S. (2001) *J. Chromatogr., A 914*, 95−103.
34. Gangl, E. T., Turesky, R. J., and Vouros, P. (2001) *Anal. Chem. 73*, 2397−2404.
35. Tretyakova, N., Matter, B., Ogdie, A., Wishnok, J. S., and Tannenbaum, S. R. (2001) *Chem. Res. Toxicol. 14*, 1058−1070.
36. Mao, B., Li, B., Amin, S., Cosman, M., and Geacintov, N. E. (1993) *Biochemistry 32*, 11785−11793.
37. Hanrahan, C. J., Bacolod, M. D., Vyas, R. R., Liu, T., Geacintov, N. E., Loechler, E. L., and Basu, A. K. (1997) *Chem. Res. Toxicol. 10*, 369−377.
38. Geacintov, N. E., Shahbaz, M., Ibanez, V., Moussaoui, K., and Harvey, R. G. (1988) *Biochemistry 27*, 8380−8387.
39. Riggs, A. D., and Jones, P. A. (1983) *Adv. Cancer Res. 40*, 1−30.
40. Tornaletti, S., and Pfeifer, G. P. (1995) *Oncogene 10*, 1493−1499.
41. Das, A., Tang, K. S., Gopalakrishnan, S., Waring, M. J., and Tomasz, M. (1999) *Chem. Biol. 6*, 461−471.
42. Mathur, P., Xu, J., and Dedon, P. C. (1997) *Biochemistry 36*, 14868−14873.
43. Denissenko, M. F., Chen, J. X., Tang, M. S., and Pfeifer, G. P. (1997) *Proc. Natl Acad. Sci. U.S.A. 94*, 3893−3898.
44. Sendowski, K., and Rajewsky, M. F. (1991) *Mutat. Res. 250*, 153−160.
45. Hertzberg, R. P., Caranfa, M. J., and Hecht, S. M. (1985) *Biochemistry 24*, 5286−5289.
46. Mathison, B. H., Said, B., and Shank, R. C. (1993) *Carcinogenesis 14*, 323−327.
47. Pradhan, P., Graslund, A., Seidel, A., and Jernstrom, B. (1999) *Chem. Res. Toxicol. 12*, 816−821.
48. Weisenberger, D. J., and Romano, L. J. (1999) *J. Biol. Chem. 274*, 23948−23955.
49. Rodin, S. N., and Rodin, A. S. (2000) *Proc. Natl Acad. Sci. U.SA. 97*, 12244−12249.
50. Basu, A. K., and Essigmann, J. M. (1988) *Chem. Res. Toxicol. 1*, 1−18.
51. Cloutier, J. F., Drouin, R., and Castonguay, A. (1999) *Chem. Res. Toxicol. 12*, 840−849.
52. Pfeifer, G. P., Denissenko, M. F., and Tang, M. S. (1998) *Toxicol. Lett. 102−103*, 447−451.
53. Funk, M., Ponten, I., Seidel, A., and Jernstrom, B. (1997) *Bioconjugate Chem. 8*, 310−317.
54. Margulis, L. A., Ibanez, V., and Geacintov, N. E. (1993) *Chem. Res. Toxicol. 6*, 59−63.

BI025540I